Journal of Research in Applied and Basic Medical Sciences 2021; 7(3): 152-160

Original Article

RABMS Journal of Research in Applied and Basic Medical Sciences

Analytical Formula for the total scatter factor of the Small Radiation Field Size

Saed J. Al Atawneh[1, 2,*]

[1] *Department of Radiation Oncology, King Hussein Cancer Center, Amman, Jordan*

[2] *Department of Physics, Faculty of Science, Al-Balqa Applied University, Jordan*

Corresponding authors:** Saed J. Al Atawneh**, Address:** Department of Radiation Oncology, King Hussein Cancer Center, Queen Rania St 202, Amman, Jordan, ***Email: saed.al-atawneh@atomki.hu, ***Tel:*** +96265300460

Abstract

***Background & Aims*:** We present an analytical formula (AF) to calculate the total scatter factor of the MLC-shaped small radiation beams.

***Materials & Methods**:* Pinpoint, Semiflex, and Farmer ion chambers were used for MLC/Jaw-shaped fields extending from (10x10 cm^2) down to (1x1 cm^2). The total scatters factor, beam profiles, and penumbra was investigated for MLC/Jaw-shaped beams.

***Results**:* We found that the total scatters factor and the penumbra was clearly higher for MLC-shaped beams due to the MLC leakage, which becomes more and more significant for the small fields. The Analytical Formula was introduced as a least-square fit equation and verified against to measure data. The maximum deviation at small field size (< 4 cm^2) was within 3.6% and 43.9% from both MLC and Jaw-shaped beams, respectively.

Conclusion: Our analytical formula shows a very good agreement with measured data at a large field size (> 4 cm^2), and had small deviation with MLC-shaped small field size, emphasizing that our analytical formula is valid and reasonably good for the total scatters factor calculation of the MLC-shaped beams, especially the ultra-small field size.

***Keywords*:** Small field dosimetry, Total Scatter Factor, Analytical Formula of Small Radiation Field Size

Received 27 December 2021; accepted for publication 11 February 2022

Introduction

Radiation therapy is a cancer treatment strategy that aims to maximize the tumor control probability (TCP) and minimize the normal tissue complication probability (NTCP) and is a reasonable achievable value utilizing ionizing radiations like x and Gammarays, and/or ionizing particles. To achieve these goals, the new techniques such as Intensity Modulated Radiation Therapy (IMRT) and Volumetric Modulated Arc Therapy (VMAT) have been established and became essential techniques in modern radiation therapy. These new strategies can be utilized to create more complex and conformal treatment plans, which can precisely depict shape of the tumor with tighter margins and reduce the toxicities to normal tissues (1).

IMRT and VMAT treatments are complex and involve many small fields because all of the fields are

[DOI: 10.52547/rabms.7.3.152]

irregularly shaped. Small radiation beams suffer from the loss of lateral electronic equilibrium. On the other hand, MLC-shaped beams suffer from leakage, which may add extra-radiation to the treated area, whilst the amount of radiation output leaving the linear accelerator at any given time depends on the field size and shape of the beam. Electronic equilibrium is a phenomenon associated with the range of secondary particles (e.g. electrons) and hence dependent on the beam energy and medium density. The electrons produced from megavoltage photon beams have a considerable range that gets prolonged in low-density media. Compared to the field size, the lateral range of the electrons is the critical parameter to the charged particle equilibrium (CPE), rather than the forward range of the electrons (2-6). The total scatters factor measurements were complicated by two concerns; the first one was the size of the ion chamber compared to the field size, and the second one was the lack of charge particle equilibrium (dis-CPE) (2, 5-8). Three distinctive ion chambers were used with various field sizes starting from 10x10 cm^2 down to 1x1 cm^2 at 10 cm depth in the water phantom for MLC/Jaw-shaped beams.

Kein et. Al. provide a description of total scatter factor measurements for small field sizes starting from 0.5x0.5 cm^2 up to 10x10 cm^2 for MLC/Jaw-shaped beams utilizing a Plastic scintillator detector (PSD) and small ion chambers (9). IAEA Technical Reports Series (TRS) No. 483 provides extensive data for the small field dosimetry using different kinds of ion chambers and detectors (10). Several studies had been discussed the small field dosimetry (1-3, 5, 6, 8, 11) using different size detectors under charged particle dis-equilibrium conditions to provide the same conclusion; the smaller the detector the better (more accurate) the total scatters factor. Along this line of thought, in this paper, we present the analytical formula to calculate the total scatters factor for MLC-shaped small radiation beams under charged particle dis-equilibrium conditions.

Materials & Methods

The linear Accelerator (Elekta Synergy, model number 151150 capable to produces three photon beams energies; 6, 10, and 15MV), linac is equipped with a multileaf collimator (MLC) used for IMRT treatments. The MLC consists of 40 pairs of tungsten alloy leaves with 7.5 cm thickness, each projecting to a 1 cm leaf width and 32.5 cm leaf length at the isocenter. The total scatter factor measurements were carried out via the Pinpoint Ion Chamber model (PTW-31023), Semiflex model (PTW-31010), and Wellhofer Farmer model (PTW-30010) ion chambers as described in Table 1.

Table 1. Characteristics of detectors used in this study.

Detectors	Detector Type	Sensitive Volume (mm)	Volume	Material
PTW 30010 wellhofer Farmer	gas filled	radius 3.05 (mm) length 23 (mm)	0.60 (cm3)	Acrylic Wall, graphited
PTW 31010 Semiflex	gas filled	radius 2.75 (mm) length 6.5 (mm)	0.125 (cm3)	Acrylic Wall, graphited
PTW 31023 Pinpoint	gas filled	radius 1.0 (mm) length 5.0 (mm)	0.015 (cm3)	Acrylic Wall, graphited

The motorized 3D water phantom (water tank) was used for total scatter factor measurements. The phantom must be "large" enough that the dimensions of the phantom ensure that a complete lateral construction is created for the desired fields.

The phantom was placed such that the surface to source distance (SSD) was 100 cm from the source. The chamber is set up within the phantom such that its axis was always parallel to the beam central axis (CAX), and the center of the ionization chamber was located at the depth of 10 cm (d=10 cm). This depth was kept constant while changing the field size of the photon beam for each measurement. Readings for the $S_{c,p}$ were taken for field sizes 10x10 cm^2 down to 1x1 cm^2 for both the

[DOI: 10.52547/rabms.7.3.152]

MLC-shaped fields with constant jaw-opening of 10x10 cm^2 and Jaw-shaped fields only. Readings were normalized to the reference field size of 10x10 cm^2.

Results

Effect of MLC on the total scatter factor:

The MLC device suffers from leakage radiation between the "leaves". As such, it is expected that this extra leakage dose would affect the total scatter factor readings as compared with the Jaw-shaped fields.

Figure 1. Shows the $S_{c,p}$ readings as a function of photon energy using Pinpoint and Farmer ion chambers. Figure 1. Also shows how the total scatters factor influenced by the field size, beam energy, and the size of the ion chamber. This emphasizes that the small chambers such as Pinpoint Ion Chamber (0.015 cm3) and low energy, in high energy beam, makes the scattering contributions become in the forwarding direction and gives appropriate readings for the total scatter factor, especially in the small radiation fields.

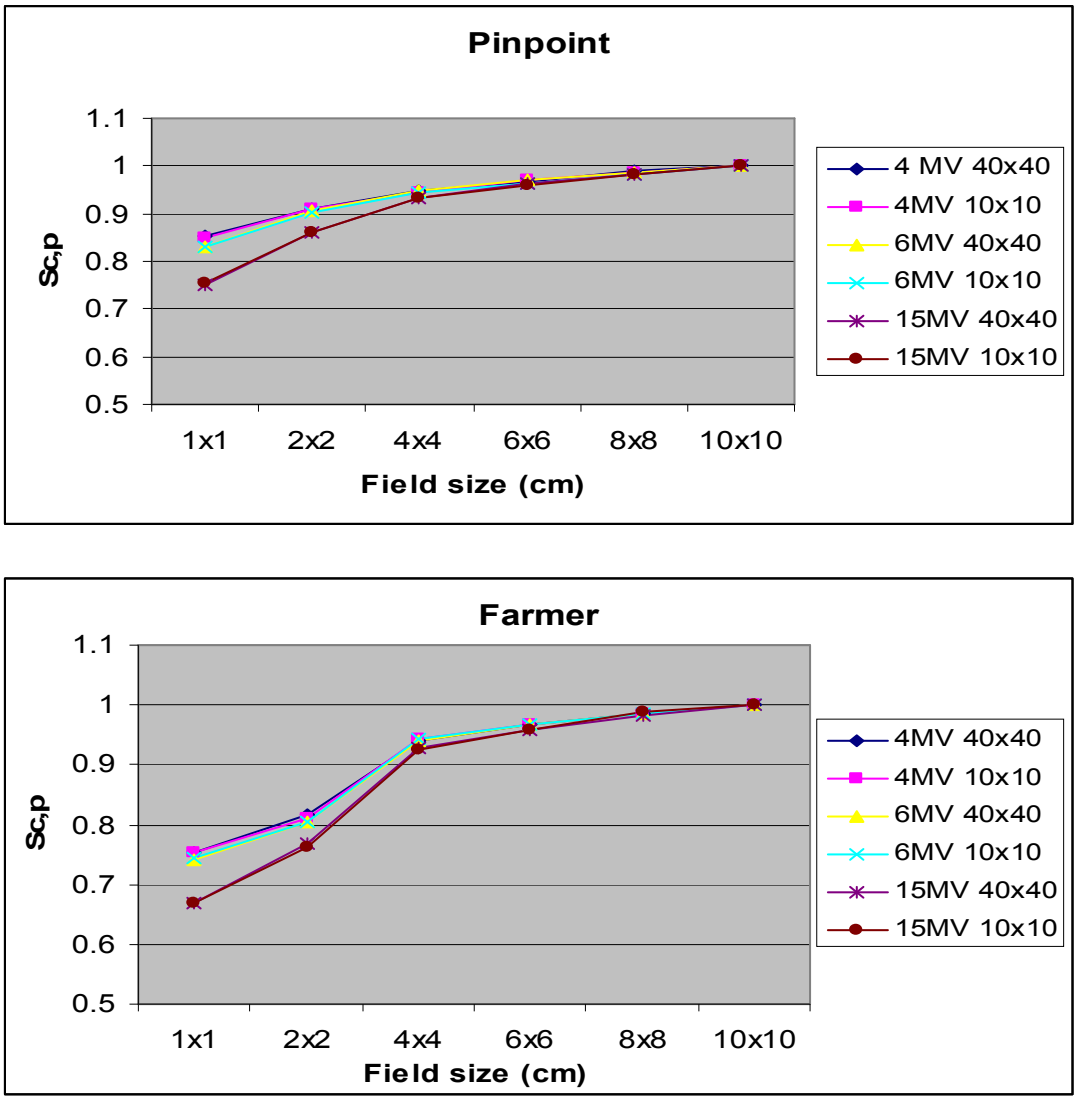

Fig 1: The Total Scatters Factor as a function of field size for two different ion chambers. Pinpoint Ion Chamber and Wellhofer Farmer Chamber at depth of 10 cm and SSD 100 cm.

Figure 2. shows that the total scatter factor (the Output Factor (OPF)) at the large fields (> 4 cm^2) for both MLC and Jaw-shaped beams data is similar (less than 2%) due to the presence of charged particle equilibrium (CPE) condition at the point of measurement (12). At small field sizes the leakage

[DOI: 10.52547/rabms.7.3.152]

through the MLC is far away from the point of measurement and the total scatter factor readings were not affected. At small field sizes (< 4 cm^2), the $S_{c,p}$ readings for both MLC and Jaw-shaped beams were highly deviated due to loss of CPE at the point of interest (2, 11).

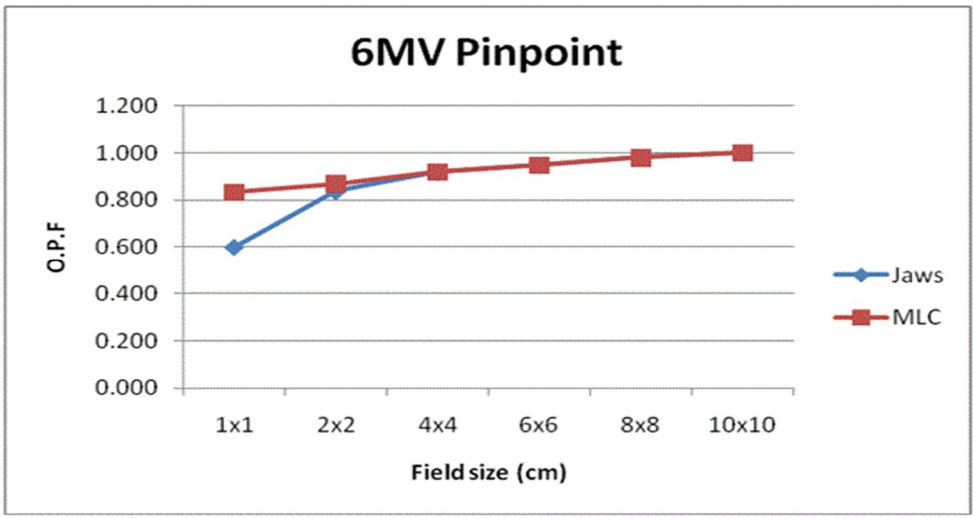

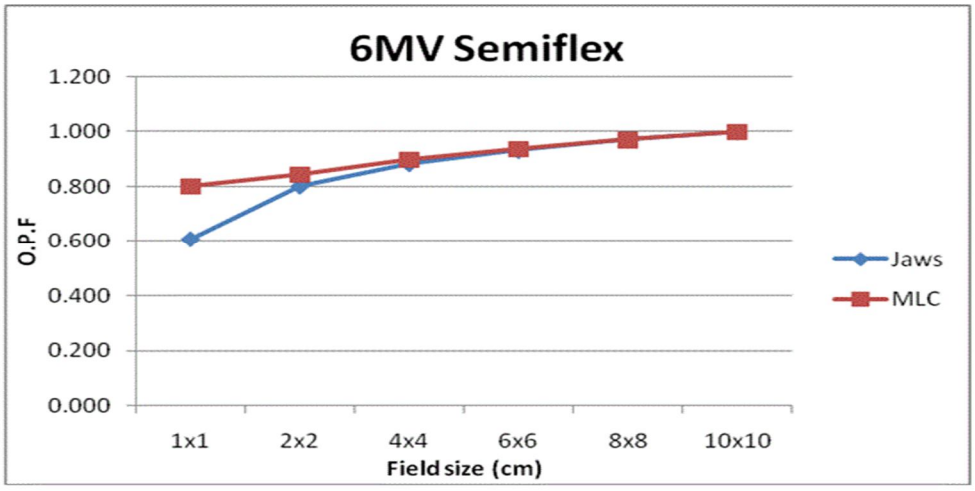

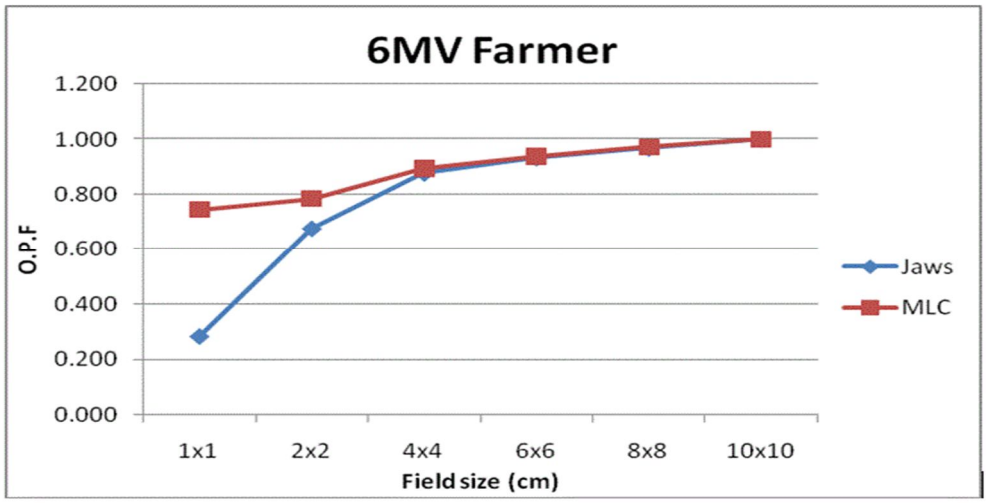

Fig 2. Total Output factor (OPF) as a function of field size for MLC/Jaw beams, 6MV beam energy using Pinpoint Ion Chamber, Semiflex Ion Chamber, and Farmer Ion Chamber. MLC = Square-red line, Jaw =Square-blue line.

[DOI: 10.52547/rabms.7.3.152]

Beam profile:

In this section, we compare the beam profiles of the jaw and the MLC device with various ion chambers. Our region of interest is the penumbra region that represents the dose fall-off outside the edges of the beam. Measurements of the beam profile were done by scanning along the center of the beam axes using Pinpoint Chamber and Semiflex Chamber for 6 MV beam energy.

Figures 3-6 show the beam profiles for both MLC and Jaw fields, and 6 MV beam energy, Pinpoint Ion Chamber, and Semiflex Ion Chamber. Figures 3-6 also shows that the transmission (leakage) through the MLC leaves increases the dose near the tail region (Penumbra) by 20% in comparison with the jaws. In addition, the inter-leaf leakage, so called tongue-and-groove, was also evident in the small "peaks" that are overlaid on the tail.

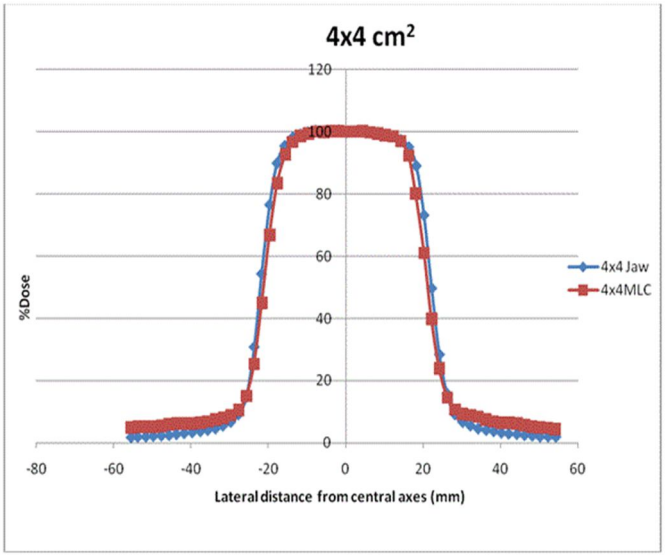

Fig 3: Shows the beam profiles for both MLC and Jaw field of 2x2 cm^2, Pinpoint Ion Chamber.

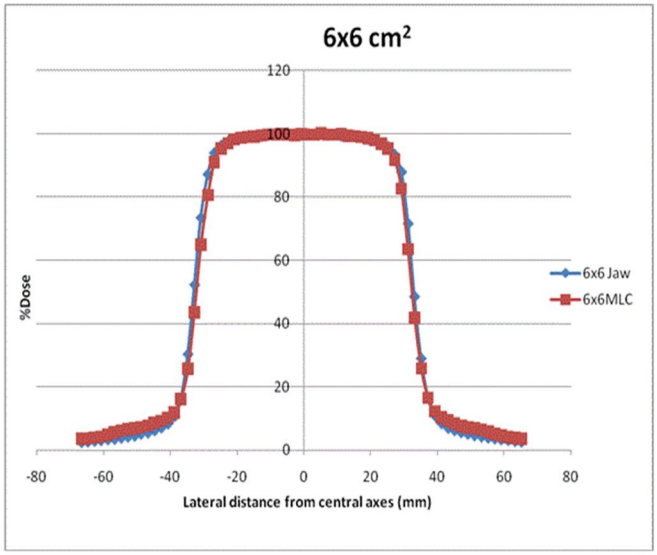

Fig 4: Shows the beam profiles for both MLC and Jaw field of 2x2 cm^2, Semiflex Ion Chamber.

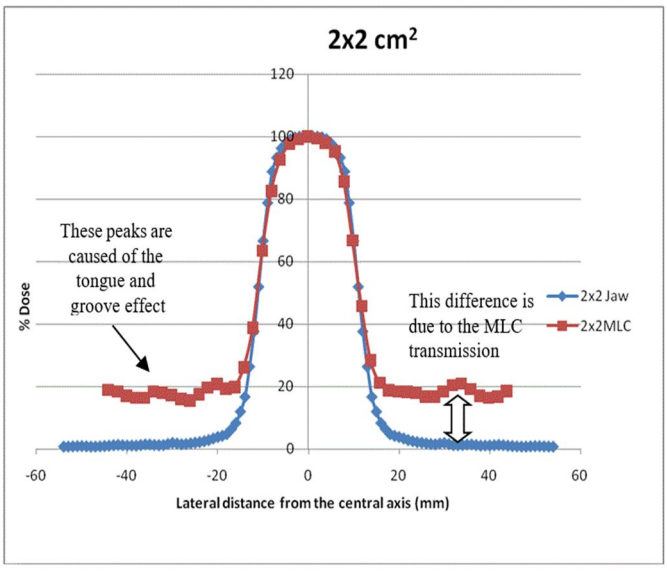

Fig 5: Shows the beam profiles for both MLC and Jaw field of 4x4 cm2, Semiflex Ion Chamber.

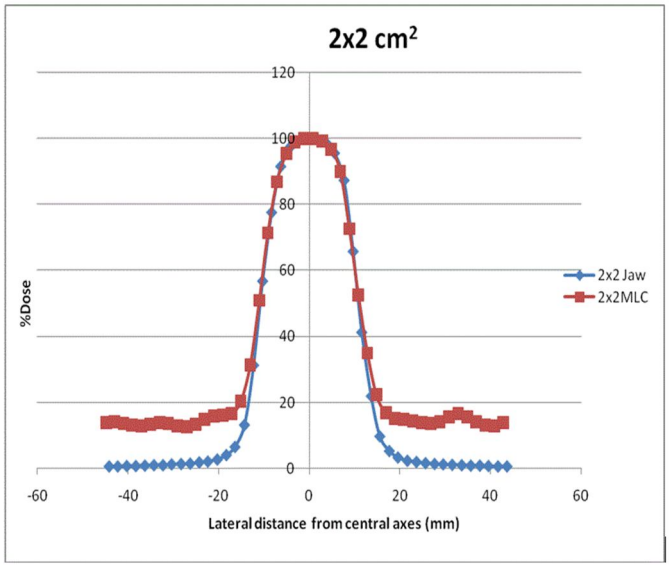

Fig 6: Shows the beam profiles for both MLC and Jaw field of 6x6 cm2, Semiflex Ion Chamber.

[DOI: 10.52547/rabms.7.3.152]

Table 2. provides penumbra readings for both MLC and Jaw-shaped beams for different field sizes. Obviously, the penumbra is affected by ion chamber size whereas the penumbra for field size 2x2 cm^2 was ranged from 4.9 mm – 10.3 mm. On the other hand, the transmission (leakage) through the MLCs, in addition to the rounded-shape of the MLC, makes the penumbra of the MLC beam profiles larger in comparison with the jaw beam profile. The effect of MLC transmission on the penumbra region becomes more pronounced as the field size decreases. For Small field size 2x2 cm^2, the percentage difference between the MLC profile's penumbra and Jaw Profile's Penumbra is the largest with 33.929% and 30.612% for the Semiflex and pinpoint, respectively.

Table 2. Penumbra for different field sizes (cm^2)

Field Size	Semiflex	Pinpoint	% Diff (Semiflex)	% Diff (Pinpoint)
6x6cm^2 Jaws	6.4	5.5	12.500	20.000
6x6cm^2 MLC	7.2	6.6		
4x4cm^2 Jaws	5.9	5.1	11.864	21.569
4x4cm^2 MLC	6.6	6.2		
2x2cm^2 MLC	5.6	4.9	33.929	30.612
2x2cm^2 Jaws	7.5	6.4		

Analytical formula of the total scatter factor:

For analytical formula, all $S_{c,p}$s were calculated based on the measured data utilizing three distinctive ion chambers through 3D-water phantom according to equation 1.

$$\Omega_{f_{clin}Q_{msr}}^{f_{clin},f_{msr}} = \frac{D_{W,Q_{clin}}^{f_{clin}}}{D_{W,Q_{msr}}^{f_{msr}}} \quad (1)$$

Where $D_{W,Q_{clin}}^{f_{clin}}$ and $D_{W,Q_{msr}}^{f_{msr}}$ are the absorbed dose to water in the clinical field f_{clin} with beam quality Q_{clin},and absorbed dose to water in the machine specific reference field f_{msr} with beam quality Q_{msr}, respectively (5, 6). Curves in figure 2 were fitted employing least-square fit "ideal" straight line for the large field sizes that could be represented by equation 2.

$$(S_{c,p}|_{Energy} = a_0 + a_1 * Field\ size\ )_{ion\ chamber} \quad (2)$$

Where a_0 and a_1 are fitting parameters that areenergy-dependent and ion chamber size independent, respectively. The first term of the analytical formula represents the total scatter factor for zero field size at given energy and the second term represents the corrected part of the total scatter factor readings under charge particle dis-equilibrium condition. Subsequently; the fitting parameters should be averaged over all ion chambers that are used for $S_{c,p}$ measurement to eliminate the ion chamber size effect under the same conditions, as described in equations 3 and 4.

$$\overline{a_0}|_E = \frac{\sum_{chamber=i} a_{0i}}{N} \quad (3)$$

And,

$$\overline{a_1}|_E = \frac{\sum_{chamber=i} a_{1i}}{N} \quad (4)$$

Where, $\overline{a_0}|_E$, $\overline{a_1}|_E$ are the average values of fitting parameters over different ion chambers.

Then, the Analytical formula (ion chamber volume-independent formula) has the following form,

[DOI: 10.52547/rabms.7.3.152]

$$S_{c,p}|_E = \overline{a_0}|_E + \overline{a_1}|_E * Field\ size \quad (5)$$

Last but not the least, the standard deviation (SD) for fitting parameters overall ion chambers at given energy should be calculated as could be seen in equations 6 and 7.

$$SD_{a_0} = \frac{\sum(a_i - \overline{a_0})^2}{N-1} \quad (6)$$

$$SD_{a_1} = \frac{\sum(a_i - \overline{a_1})^2}{N-1} \quad (7)$$

Experiment Validation:

The Analytical Formula for the total scatters factor was validated and compared with measured data for both MLC and Jaw-shaped beams. Tables 3 to 5 compare total scatter factors computed using an analytical formula to those observed using ion chambers for both MLC and Jaw-shaped field sizes.

Table 3: The Analytical Formula Readings vs Measured Readings for 6MV beam, measured with Pinpoint Ion Chamber at depth of 10 cm of SSD 100 cm.

Pinpoint					
Field size (cm2)	Measured OF MLC	Measured OF Jaws	Analytical	diff (MLC)	diff (Jaws)
10	1	1	1	0	0
8	0.98	0.98	0.98	0	0
6	0.947	0.947	0.947	0	0
4	0.917	0.917	0.917	0	0
2	0.868	0.835	0.891	0.023	0.056
1	0.832	0.599	0.862	0.030	0.263

Table 4: The Analytical Formula Readings vs Measured Readings for 6MV beam, measured with Semiflex Ion Chamber at depth of 10 cm of SSD 100 cm**.**

Semiflex					
Field size (cm2)	Measured OF MLC	Measured OF Jaws	Analytical	diff (MLC)	diff (Jaws)
10	1	1	1	0	0
8	0.972	0.971	0.972	0	0.001
6	0.938	0.932	0.938	0	0.006
4	0.899	0.885	0.899	0	0.014
2	0.843	0.803	0.868	0.025	0.065
1	0.801	0.609	0.834	0.033	0.225

[DOI: 10.52547/rabms.7.3.152]

Table 5: The Analytical Formula Readings vs Measured Readings for 6MV beam, measured with Farmer ion chamber at depth of 10 cm of SSD 100 cm.

Farmer					
Field size (cm2)	Measured OF MLC	Measured OF Jaws	Analytical	diff (MLC)	diff (Jaws)
10	1	1	1	0	0
8	0.973	0.968	0.973	0	0.005
6	0.939	0.933	0.939	0	0.006
4	0.895	0.877	0.895	0	0.018
2	0.784	0.676	0.865	0.081	0.189
1	0.745	0.281	0.830	0.085	0.549

Tables 3 to 5 show the "Analytical Formula Calculations" for the ideal straight lines based on the equation (5). The last two columns show the difference between linear value and the MLC/Jaw values where the deviation of the straight line indicates the amount of charged particle equilibrium losses. The total scatter factors of the small filed size less than 1x1 cm^2 for the smallest ion chamber (pinpoint) is deviated by 3.6% and 43.9% from analytical formula readings for MLC and Jaw-shaped beams sequentially and followed by 2.6% and 6.7% for field size 2x2 cm^2 for MLC and Jaw-shaped beams, respectively. For the Semiflex Ion Chamber, the OFs of the small filed size less than 1x1 cm^2 are deviated by 3.95% and 26.97% from analytical formula readings for MLC and Jaw-shaped beams and followed by 22.8% and 7.48% for field size 2x2 cm^2 for MLC and Jaw-shaped beams, respectively. whilst the worst-case scenario occurred with the Farmer ion chamber, the total scatter factors of the small filed size less than 1x1 cm^2 are deviated by 10.2% and 9.3% from analytical formula readings for MLC and Jaw-shaped beams, and followed by 66.14% and 21.8% for field size 2x2 cm^2 for MLC and Jaw-shaped beams, sequentially. As noticed, the smallest deviation was recorded by Pinpoint Ion Chamber for MLC-shaped beam (1x1 cm^2) with 3.6% followed by the Semiflex Ion Chamber with 3.65% compared to the largest ion chamber (Farmer) with 10.2%. These differences wer due to the volume averaging effect of ion chambers, which clearly appeared at the ultra-small field size “i.e. smaller than 1.5 cm^2”.

Discussion & Conclusion

We presented a correct Analytical Formula to calculate the total scatter factors. The Analytical Formula was verified against to measure data. Our results for the Pinpoint Ion Chamber, the smallest ion chamber in this study, show a maximum deviation of 3.6% and 43.9% for MLC and Jaw-shaped beams, respectively. We found that the total scatters factor for MLC-shaped beams at the small field sizes less than 4x4 cm^2 was higher than Jaw-shaped beams; this was expected due to interleaf leakage that adds to the radiation reaching the point of measurement. The total scatter factors for large field size, (e.g. larger than 4x4 cm^2) were almost the same for both MLC/Jaw-shaped beams with a maximum deviation of less than 2%. We also investigated all factors that might influence the penumbra such as the field size, ion chamber volume, and radiation beam energy, especially for the small field size (2x2cm^2). We found that the analytical formula that we presented could be reasonably useful to calculate the total scatter factor with a standard deviation of less than 5%, and also strongly recommended to use it for the commission data in cases that the small detectors such as pinpoint, micro-diamond, or even diode detectors do not achievable to use.

[DOI: 10.52547/rabms.7.3.152]

Conflict of interest

The authors declare no financial or other conflict of interest.

References

1. Masanga W, Tangboonduangjit P, Khamfongkhruea C, Tannanonta C. Determination of small field output factors in 6 and 10 MV flattening filter free photon beams using various detectors. J. Phys. Conf. Ser 2016;694:012027.
2. Das IJ, Ding GX, Ahnesjo A. Small fields: nonequilibrium radiation dosimetry. Medical physics 2008;35(1):206-15.
3. Charles PH, Cranmer-Sargison G, Thwaites DI, Crowe SB, Kairn T, Knight RT, et al. A practical and theoretical definition of very small field size for radiotherapy output factor measurements. Medical physics 2014;41(4):041707.
4. Klein DM, Tailor RC, Archambault L, Wang L, Therriault-Proulx F, Beddar AS. Measuring output factors of small fields formed by collimator jaws and multileaf collimator using plastic scintillation detectors. Medical physics 2010;37(10):5541-9.
5. Zhu TC, Ahnesjö A, Lam KL, Li XA, Ma C-MC, Palta JR, et al. Report of AAPM Therapy Physics Committee Task Group 74: In-air output ratio, , for megavoltage photon beams. Medical physics 2009;36(11):5261-91.
6. Huq MS, Hwang M-S, Teo TP, Jang SY, Heron DE, Lalonde RJ. A dosimetric evaluation of the IAEA-AAPM TRS483 code of practice for dosimetry of small static fields used in conventional linac beams and comparison with IAEA TRS-398, AAPM TG51, and TG51 Addendum protocols. Medical physics 2018;45(9):4257-73.
7. Laub WU, Wong T. The volume effect of detectors in the dosimetry of small fields used in IMRT. Medical physics 2003;30(3):341-7.
8. Francescon P, Cora S, Cavedon C. Total scatter factors of small beams: a multidetector and Monte Carlo study. Medical physics 2008;35(2):504-13.
9. Klein DM, Tailor RC, Archambault L, Wang L, Therriault-Proulx F, Beddar AS. Measuring output factors of small fields formed by collimator jaws and multileaf collimator using plastic scintillation detectors. Medical physics 2010;37(10):5541-9.
10. Palmans H, Andreo P, Huq MS, Seuntjens J, Christaki KE, Meghzifene A. Dosimetry of small static fields used in external photon beam radiotherapy: Summary of TRS-483, the IAEA–AAPM international Code of Practice for reference and relative dose determination. Medical physics 2018;45(11):e1123-e45.
11. Sauer OA, Wilbert J. Measurement of output factors for small photon beams. Medical physics. 2007;34(6):1983-8.
12. Hrbacek J, Lang S, Klock S. Commissioning of photon beams of a flattening filter-free linear accelerator and the accuracy of beam modeling using an anisotropic analytical algorithm. Int. J. Radiat. Oncol. Biol. Phys 2011;80(4):1228-37.

[DOI: 10.52547/rabms.7.3.152]